Clays and Clay Minerals, Vol. 62, No. 1, 62–73, 2014.

DIELECTRIC RELAXATION OF WATER IN CLAY MINERALS

Maria A. Vasilyeva[1], Yuri A. Gusev[1,*], Valery G. Shtyrlin[2], Anna Greenbaum (Gutina)[3], Alexander Puzenko[3], Paul Ben Ishai[3], and Yuri Feldman[3]

[1] The Kazan Federal University, Institute of Physics, Kremlevskaya st. 18, 420008, Kazan, Russian Federation
[2] The Kazan Federal University, A.M. Butlerov Chemistry Institute, Kremlevskaya st. 18, 420008, Kazan, Russian Federation
[3] The Hebrew University of Jerusalem, Department of Applied Physics, Edmond J. Safra Campus, Givat Ram 91904, Jerusalem, Israel

Abstract—The study of confined water dynamics in clay minerals is a very important topic in aluminosilicate-surface chemistry. Aluminosilicates are among the most technologically versatile materials in industry today. Dielectric spectroscopy is a very useful method for investigating the structure and dynamics of water adsorbed on solid matrix surfaces and water in the vicinity of ions in solutions. Use of this method for the study of clay minerals has been underutilized to date, however. The main goal of the present research was to understand the relaxation mechanisms of water molecules interacting with different hydration centers in clay minerals, with a view to eventually control this interaction. Two types of natural layered aluminosilicates (clay minerals) – montmorillonite with exchangeable K^+, Co^{2+}, and Ni^{2+} cations and kaolinite with exchangeable K^+ and Ba^{2+} cations – were examined by means of dielectric spectroscopy over wide ranges of temperature (from −121ºC to +300ºC) and frequency (1 Hz–1 MHz). An analysis of the experimental data is provided in terms of four distributed relaxation processes. The low-temperature relaxation was observed only in montmorillonites and could be subdivided into two processes, each related to a specific hydration center. The cooperative behavior of water at the interface was observed in the intermediate temperature region, together with a proton percolation. The dielectric properties of ice-like and confined water structures in the layered clay minerals were compared with the dielectric response observed in porous glasses. The spatial fractal dimensions of the porous aluminosilicates were calculated by two separate methods – from an analysis of the fractality found in photomicrographs and from the dielectric response.

Key Words—Adsorbed Water, Dielectric Spectroscopy, Exchangeable Cations, Fractal Dimension, Kaolinite, Montmorillonite.

INTRODUCTION

The large specific surface area, chemical and mechanical stability, variety of structural and surface properties, large values of cation exchange capacities, *etc.*, make the clay minerals an excellent group of adsorbents (Greg and Sing, 1967; Gupta and Bhattacharyya, 2012; Kiselev, 1986; Tarasevich, 1988; Tarasevich and Ovcharenko, 1975; Volzone *et al.*, 1999). Consequently, the hydration properties of clay materials are a fundamental problem in any field of their application.

One of the most useful tools for investigating the structure and dynamics of adsorbed water on solid matrix surfaces is Dielectric Spectroscopy (DS) (Gutina *et al.*, 2003; Saltas *et al.*, 2007; Spanoudaki *et al.*, 2005; Wander and Clark, 2008). Broadband Dielectric Spectroscopy (or impedance spectroscopy) occupies a special place among the numerous modern methods used for the physical and chemical analysis of materials. By measuring the electric polarization of a dielectric material under the influence of an external time-dependent electric field at different temperatures, investigation of relaxation processes with an extremely wide range of characteristic times (10^5–10^{-13} s) and monitoring different scales of molecular motions are possible (Kremer and Schoenhals, 2002; Feldman *et al.*, 2006). In particular, DS is sensitive to cooperative intermolecular interactions (Feldman *et al.*, 2006) and, thus, provides a link between the properties of the individual constituents of a complex material *via* molecular spectroscopy and the characterization of its bulk properties. Many key aspects of a material's properties can be derived from the complex dielectric functions, *e.g.* the strength and the shape parameters of molecular relaxations, the characterization of structural phase transitions, the activation energy of the relaxation process, charge mobility, *etc*. Moreover, this method is very sensitive to water dynamics in ionic aqueous solutions and can provide important information on the state of water in the vicinity of ions (Levy *et al.*, 2012).

The clay minerals represent a class of materials where the two types of water organization mentioned above can be observed simultaneously. Several attempts have been made to perform dielectric measurements of hydrated kaolinites and montmorillonites over narrow frequency and temperature ranges by changing the temperature at a fixed frequency or *vice versa* (Calvet, 1975; Hall and Rose, 1978; Hoekstra and Doyle, 1971; Lockhart, 1980a, 1980b; Mamy, 1968; Raythatha and Sen, 1986; Sposito

* E-mail address of corresponding author:
ygusev@mail.ru
DOI: 10.1346/CCMN.2014.0620106

and Prost, 1982). Recently, the increased interest in hydrated clay minerals has stimulated research in this field, primarily to correlate the electrical properties with their structural parameters and water content (Ishida *et al.*, 2000; Kaviratna *et al.*, 1996; Logsdon and Laird, 2002, 2004; Rotenberg *et al.*, 2005). The main aim of the present study was to examine the effect of various types of cations on the dielectric response of hydrated montmorillonite and kaolinite clay minerals over broad ranges of temperature (from −121ºC to +300ºC) and frequency (1 Hz−1 MHz), in order to obtain detailed information on the structure and the relaxation properties of water adsorbed by different hydration centers in the minerals. Preliminary results of the work were published by Vasilyeva *et al.* (2012a, 2012b).

EXPERIMENTAL

Materials

Two types of clay minerals were considered here: Oglanlinsky montmorillonite (from Turkmenistan) and Glukhovetsky kaolinite (from Ukraine). The clay minerals were treated in the Laboratory of Disperse Systems of the Institute of Colloid and Water Chemistry (Kiev, Ukraine) according to a procedure described by Tarasevich and Ovcharenko (1975, 1980). At first, impurities of other minerals, free oxides and hydroxides of Fe and Al, as well as other impurities and inclusions were removed from the raw clay. To obtain the purest samples possible, 3−5% aqueous suspensions of the clay mineral in question were mixed thoroughly until no agglomerates were visible and then kept at quiescence for ~30 min. A method of separating the solid clay particles from the liquid was chosen to elutriate the finest fraction: the precipitate was allowed to settle and the liquid settled or carefully decanted or filtered off through a siphon (Tarasevich and Ovcharenko, 1975, 1980). For kaolinite no other treatment was performed. Additional purification and centrifugation were required for montmorillonites. The purity (homogeneity) of the samples was checked by X-ray diffraction (XRD) and infrared (IR) spectroscopy. Then cleaned natural samples were treated 7−8 times with a 1 M NaCl solution at a solid:liquid (S:L) ratio of 1:20; each time the system was shaken, kept at quiescence for ~1 h, and then decanted. Afterward, the Na-saturated minerals were washed free of excess salts using distilled water. (resistivity not measured). Next, the clay minerals were treated 7−8 times in the same way with 1 N solutions of the required metal chlorides (KCl, $BaCl_2$, $CoCl_2$, $NiCl_2$) in the same S:L ratio. Finally, the samples were washed with distilled water until a negative reaction for chloride ion (with $AgNO_3$), dried for ~1 h at ~100ºC in air, then dried for ~1 h at ~50ºC in vacuum, and then stored at ambient air humidity until measured.

Table 1. Relative water content, h, in the samples studied.

Sample	h (%)
K-montmorillonite	13.7
Ni-montmorillonite	14.7
Co-montmorillonite	15.3
K-kaolinite	2.3
K,Ba-kaolinite	5.4

The relative water content, h, was determined by weighing the samples prior to and immediately after the dielectric measurements according to equation 1. The water content in a sample was calculated as a percent weight of the sample relative to the initial weight (Table 1):

$$h\ (\%) = 100 \times (m_{\text{initial}} - m_{\text{final}})/m_{\text{initial}} \qquad (1)$$

Methods

The elemental composition of the samples was determined by X-ray fluorescence (XRF) analysis, using an energy dispersive X-ray spectrometer EDX 800HS2 (Shimadzu, Germany) (Table 2).

The morphology of the samples was examined using a field emission scanning electron microscope (FESEM) (Merlin, Carl Zeiss, Germany). Images of the morphology of some of the samples were collected using FESEM (Figure 1).

Powder XRD measurements were performed at room temperature using a D8 Advance diffractometer (Bruker AXS, Karlsruhe, Germany) with a goniometer radius of 217.5 mm, Göbel Mirror parallel-beam optics, 2º Sollers slits, and 0.2 mm receiving slit. Profile fitting, refinement of unit-cell parameters, and crystallite-size calculations were performed using the *EVA* software (Bruker, AXS). The crystallite sizes of monoclinic Ni- and Co-montmorillonite obtained were 251.5 Å and 199.1 Å, respectively; the crystallite size of triclinic kaolinite was

Table 2. Elemental compositions of the four studied samples.

Sample	Mg (%)	Al (%)	Si (%)	K (%)	Ti (%)	V (%)	Fe (%)	Ni (%)	Cu (%)	Zn (%)	Ba (%)
K-montmorillonite	1.8	11.3	74.7	8.7	0.4		2.9		0.2	0.1	
Ni-montmorillonite	2.4	13.6	71.5		0.5		3.1	8.5	0.4		
K-kaolinite		35.5	57.5	2.9	1.9	0.1	1.9			0.1	
K,Ba-kaolinite		37.0	57.3	1.0	2.3		1.2		0.1	0.1	1.0

https://doi.org/10.1346/CCMN.2014.0620106 Published online by Cambridge University Press

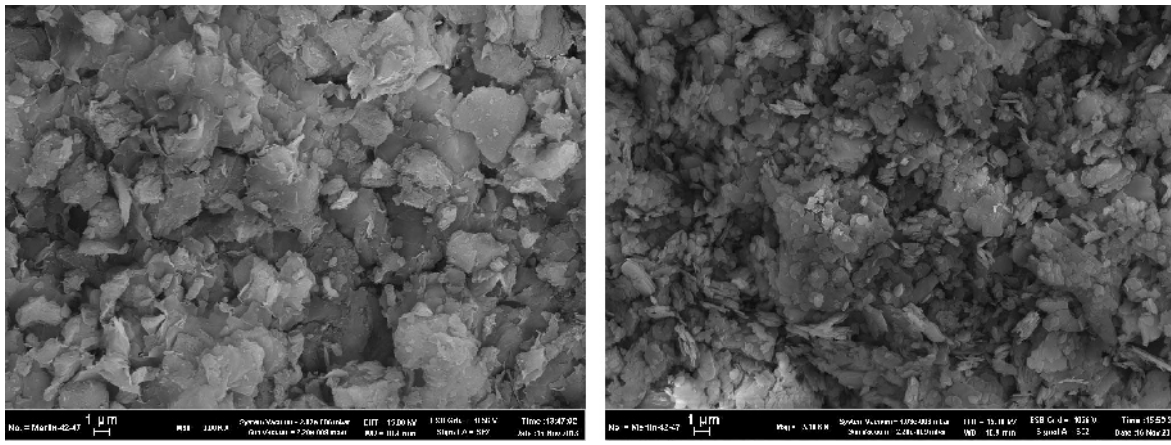

Figure 1. Electron micrographs of Ni-montmorillonite (left) and K-kaolinite (right).

382.7 Å. The kaolinite sample also contained some monoclinic sericite with a crystallite size of 409.1 Å.

Dielectric measurements in the frequency range of 1 Hz−1 MHz were performed using a BDS 80 Dielectric Spectrometer, based on an Alpha Impedance Analyzer (Novocontrol, Germany) with automatic temperature control by a Quatro Cryosystem, with a precision of 0.5ºC. The Alpha High Resolution Dielectric Analyzer can measure impedances from 10^{-2} to 10^{14} Ohms with a resolution in loss factor $\tan(\delta)<10^{-5}$ (Schaumburg, 1994; Kremer and Schoenhals, 2002). A voltage U_0 with a fixed frequency is applied to the cell which contains the material under investigation. The resulting current, I_0, has the same frequency but a phase shift between current and voltage described by the phase angle, φ. The ratio of U_0 and I_0 and the phase angle φ is determined from the electromagnetic and the geometric properties of the sample. The formulae for the voltage $U(t)$ and current $I(t)$ in their phasor notations can be represented conveniently by the following:

$$U(t) = U_0 \sin(\omega t) = I_m(U^* \exp(i\omega t))$$
$$I(t) = I_0 \sin(\omega t + \varphi) = I_m(I^* \exp(i\omega t)) \quad (2)$$

where $U^* = U' + iU'' = U_0$; $I^* = I' + iI''$; $I_0 = \sqrt{(I'^2 + I''^2)}$; $\tan(\varphi) = I''/I'$ where i is the imaginary unit and ω is the cyclic frequency. For a material with a linear electromagnetic response, the measured complex impedance of the sample capacitor is

$$Z^*(\omega) = Z' + iZ'' = U^*/I^* \quad (3)$$

This is related to the complex dielectric permittivity of the sample material by:

$$\varepsilon^*(\omega) = \varepsilon'(\omega) - i\varepsilon''(\omega) = \frac{1}{i\omega C_0}\frac{1}{Z^*(\omega)} \quad (4)$$

where $\varepsilon^*(\omega)$ is the complex dielectric permittivity, $\varepsilon'(\omega)$ and $\varepsilon''(\omega)$ are real and imaginary parts, respectively, of the $\varepsilon^*(\omega)$, and C_0 is the empty cell capacity.

A parallel plate capacitor with electrodes of 16 mm diameter and a spacing of ~0.5 mm between them was used. The study was carried out using the following protocol: Each of the samples was placed in the sample cell at room temperature and the measurements were then performed by quenching the samples down to −115ºC. Then the samples were measured upon heating to −58ºC with 3ºC intervals and then at intervals of 6ºC up to +300ºC. Afterward, annealing was performed inside the cryostat at 300ºC for 3 h. For montmorillonite with Co^{2+} as the exchangeable cation, the lowest temperature was −121ºC. After annealing, the samples were cooled to 25ºC and stored at this temperature in a nitrogen atmosphere until weighing. The montmorillonite samples with K^+ and Ni^{2+} as the exchangeable cations were also measured during the decrease in temperature down to 25ºC, in order to check the reversibility of the signal. All samples were weighed prior to and immediately after the experiments. The accuracy of the complex dielectric permittivity was better than 3%.

RESULTS

The complex non-Debye dielectric behavior of the clay minerals (Figures 2 and 3) can be described in terms of several distributed relaxation processes, separated by different frequency and temperature intervals, and marked as I−IV, according to their appearance during the heating experiment.

At low temperatures from −121ºC to −75ºC, the spectra of montmorillonites consisted of two relaxation processes marked I.1 and I.2, respectively (Figure 4). Both of these processes are characterized by a strong temperature dependence. In the kaolinite samples measured with the same protocol, the low-temperature process I was absent.

In the mid-temperature range from −90ºC to +150ºC, a relaxation process with a specific saddle-like shape and distinctive kink point was observed for mont-

https://doi.org/10.1346/CCMN.2014.0620106 Published online by Cambridge University Press

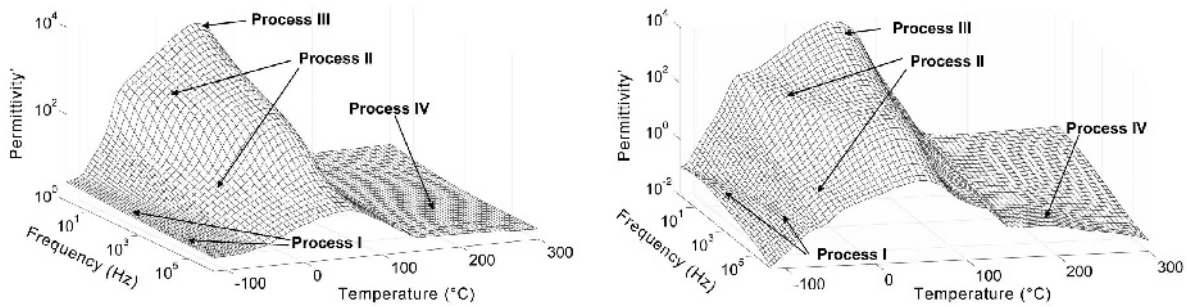

Figure 2. Typical 3D plots of the frequency and temperature dependences of the dielectric permittivity (left) and dielectric losses (right) for Ni-montmorillonite.

morillonite clay minerals at different frequency-temperature intervals simultaneously, while only one relaxation process, II, was observed in the case of kaolinite samples (Figure 5).

Relaxation process III was detected at temperatures from −50ºC to +70ºC for montmorillonites and from −70ºC to +40ºC for kaolinites. When viewed in an *ac*-conductivity presentation ($\sigma_{ac}(\omega)=(i\omega\varepsilon^*(\omega))$), typical *s*-like behavior of the low-frequency conductivity demonstrates the percolative nature of this process (Figure 6).

The amplitude of process III essentially decreased when the frequency increased and the maximum of the dielectric permittivity and losses *vs.* temperature had no temperature dependence (Figure 7) for all the clay-mineral samples.

The percolation temperature point, T_p, was determined by the maximum of the temperature dependence of the dielectric permittivity at the lowest measured frequency. The percolation temperature for montmorillonites was greater than for kaolinites (Table 3).

When the temperature rose above 100ºC, the samples became more electrically conductive. The relaxation processes were overlapped in the dielectric losses by a *dc*-conductivity. Some were even screened by the conductivity (Figure 8). A detailed investigation of the high-temperature region is the subject of a separate study.

After annealing the samples, the 3D plots of the dielectric losses *vs.* frequency and temperature changed dramatically (Figure 9). The relaxation processes previously observed in the mid-temperature window disappeared. Traces of the high-temperature spectrum were observed during the cooling measurement (Figures 8 and 9).

DISCUSSION

As shown above, all the samples lost some mass during the experiment. The clay-mineral samples demonstrated the absence of the dielectric relaxation processes at low- and mid-temperature levels after heating for extended periods of time at 300ºC (Figures 2, right and 9). As mentioned above, clay materials can adsorb water easily at their surfaces and around exchangeable cations, suggesting that water is the origin of the dielectric relaxation in these materials in the low- and mid-temperature intervals. Note that a similar conclusion was reported for porous glass systems (Gutina *et al.*, 2003).

From a structural point of view, the surface of the broken edges of the mineral layer has primary broken Al−O and Si−O bonds, resulting in polar sites. Water molecules form hydrogen bonds with surface oxygen atoms and exchangeable cations, to create new water structures very different from those of the bulk (Schoonheydt and Johnston, 2006; Sposito and Prost, 1982). In confined spaces or near interfaces, water forms distinctively layered structures with a restriction of water molecular mobility (Behnsen and Faulkner, 2011).

The minerals studied differ in their surface properties and exchangeable cations due to the differences in mineralogy and crystal structure, which lead to the variation in their affinity toward water.

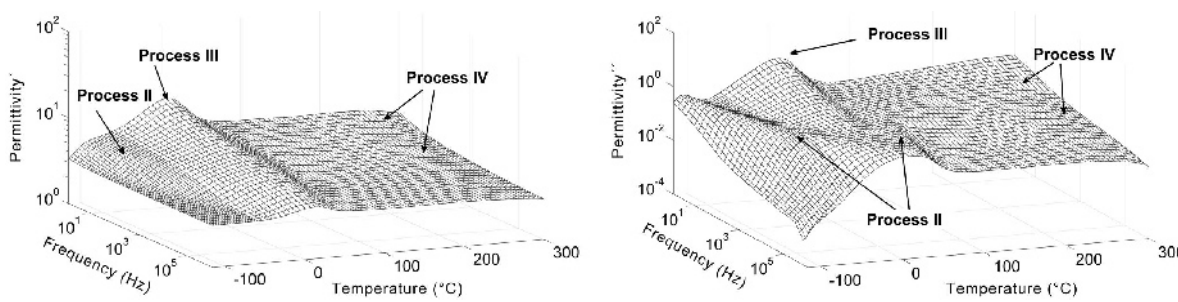

Figure 3. Typical 3D plots of the frequency and temperature dependences of the dielectric permittivity (left) and dielectric losses (right) for K-kaolinite.

https://doi.org/10.1346/CCMN.2014.0620106 Published online by Cambridge University Press

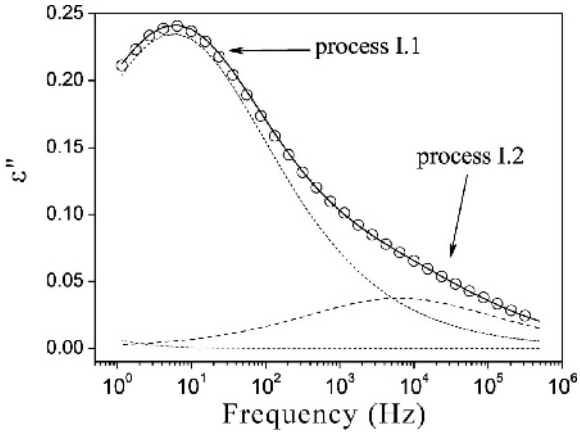

Figure 4. Measured dielectric losses *vs.* frequency at −121ºC for Co-montmorillonite. The dashed lines mark two Cole-Cole and Jonscher terms used for fitting the experimental data (open circles). The solid line is the superposition of the terms above.

The low-temperature dielectric relaxation

In the low-temperature interval (from −121ºC to −75ºC) the dielectric relaxation process (I) was observed for montmorillonites only. Therefore, this process must be associated with the relaxations of interlayer water molecules which are absent from kaolinites. Moreover, the dielectric spectrum of montmorillonites consists of two low-temperature relaxation processes (Figure 4).

Whenever water interacts with another dipolar or charge entity, a broadening of its Debye dielectric relaxation spectra occurs (Puzenko *et al.*, 2010; Levy *et al.*, 2012). In most cases this broadening can be described by the phenomenological Cole-Cole (CC) spectral function (Cole and Cole, 1941):

$$\varepsilon^*(\omega) = \varepsilon_\infty + \frac{\Delta\varepsilon}{1 + (i\omega\tau)^\alpha} \qquad (5)$$

where $\Delta\varepsilon = \varepsilon_s - \varepsilon_\infty$ is the dielectric strength of the relaxation process; ε_s and ε_∞ are the low- and high-frequency limits of the complex dielectric permittivity, respectively; τ is a characteristic relaxation time; and the exponent α is referred to as a measure of symmetrical broadening in the dielectric losses relaxation peak ($0<\alpha\leqslant 1$). A fruitful approach has been the application of fractional calculus to uncover a physical mechanism underlying the CC behavior in complex systems (Puzenko *et al.*, 2010; Levy *et al.*, 2012; Puzenko *et al.*, 2012). Taking into account that both low-temperature processes (I.1 and I.2) of montmorillonites are associated with the interaction of the water dipoles with the clay's mineral matrix, the quantitative analysis of the isothermal dielectric spectra uses a superposition of two CC functions, and an empirical Jonscher (J) term is convenient (Jonscher, 1996) (Figure 4):

$$\varepsilon^*(\omega) = \varepsilon_\infty + \sum_{j=1}^{2} \frac{\Delta\varepsilon_j}{1 + (i\omega\tau_j)^{\alpha_j}} + B \cdot (i\omega)^{n-1} \qquad (6)$$

where j denotes the number of the corresponding relaxation process and n is a Jonscher parameter for the high-frequency part of the respective relaxation process.

The temperature dependences of the relaxation times for the observed low-temperature processes demonstrated Arrhenius behavior (Figure 10). The activation energies of the low-temperature relaxation processes were then calculated (Table 4).

In montmorillonites the water molecules responsible for the low-temperature relaxations are located near the

Table 3. Values of the percolation temperature for the clay minerals studied.

Sample	T_p (ºC)
K-montmorillonite	40
Co-montmorillonite	40
Ni-montmorillonite	35
K-kaolinite	8
K,Ba-kaolinite	8

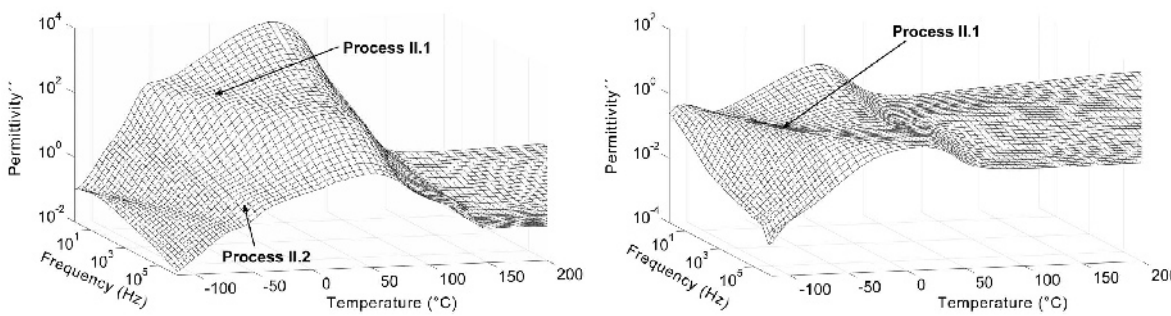

Figure 5. Typical 3D plots of the frequency and temperature behavior of the dielectric losses at a mid-temperature interval for Ni-montmorillonite (left) and K-kaolinite (right).

https://doi.org/10.1346/CCMN.2014.0620106 Published online by Cambridge University Press

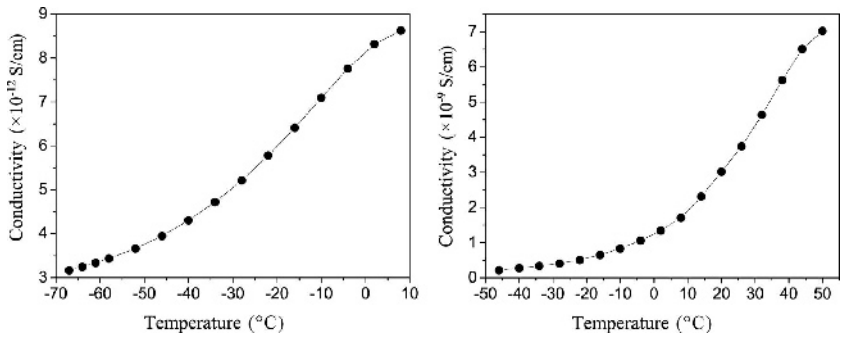

Figure 6. Temperature behavior of the low-frequency conductivity for Ni-montmorillonite (left) and K-kaolinite (right) in the mid-temperature region.

inner hydrophilic centers of interlayer channels (siloxane bonds and trapped cations) and around the interlayer cations (Salles *et al.*, 2008; Tarasevich and Ovcharenko, 1975). This is reflected by the formation of two types of structure in the low-temperature region. The slower relaxation process I.1 almost coincides with the low-temperature relaxation behavior of water adsorbed in porous silica glasses (Gutina *et al.*, 2003) (Figure 10). The activation-energy values of this process for montmorillonite samples are in the same range as that reported earlier for the porous glass materials (Gutina *et al.*, 2003; Ryabov *et al.*, 2001). The I.1 relaxation process was assumed, therefore, to correspond to ice-like water structures formed on the interior surface of interlayer channels. The second, faster, relaxation process I.2 reflects the water structures near the hydrated cations located in the interlayer channels. Thus, the nature of the hydration center plays an important role in the water dynamics of the adsorbed water in inorganic materials. Note that the type I.2 process in the glass materials (Gutina *et al.*, 2003) was not observed, but only one type of hydration center was observed in those materials. In both processes (I.1 and I.2) the activation energy depended on the type of interlayer cations and on the water content (Table 4). The detailed dielectric investigation of the formation of hydrated clusters and their structures as a function of the exchangeable cations and water content in the montmorillonites will be reported in a future study.

The mid-temperature relaxation process

Saddle-like relaxation processes were observed in the mid-temperature range from −90ºC to +150ºC for all the samples studied. Quantitative analysis of the mid-temperature relaxation process was performed based on the model described by Gutina *et al.* (2003) in which the

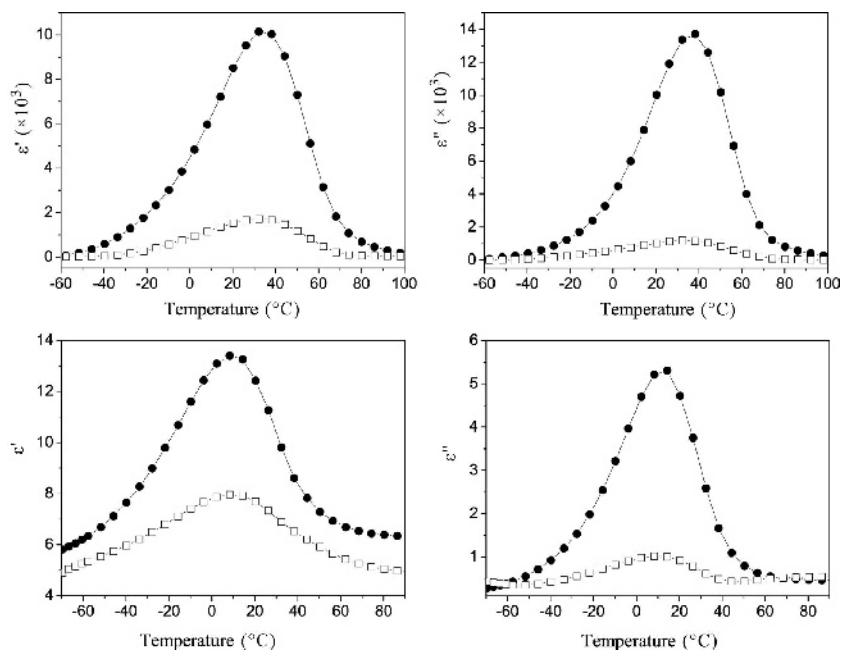

Figure 7. Typical temperature behavior of the dielectric permittivity (left) and dielectric losses (right) at percolation for Ni-montmorillonite (upper) and K-kaolinite (lower) at frequencies of 1 Hz (●) and 133 Hz (□).

https://doi.org/10.1346/CCMN.2014.0620106 Published online by Cambridge University Press

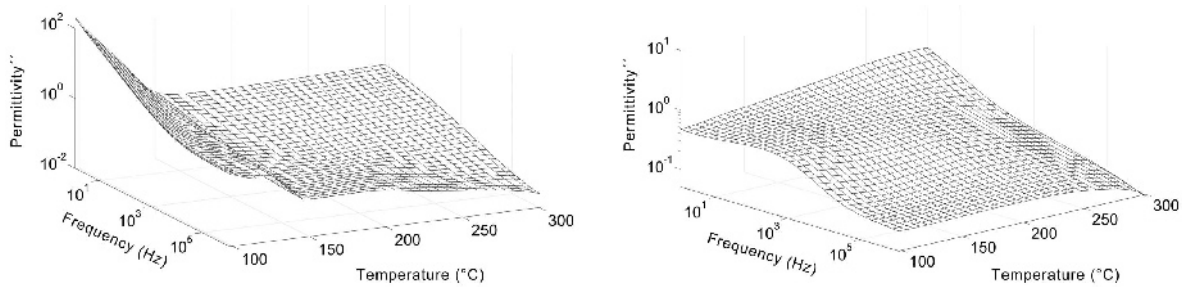

Figure 8. Typical 3D plots of the frequency and temperature dependences of the dielectric loss at high temperatures plotted for Ni-montmorillonite (left) and K-kaolinite (right).

act of relaxation was considered to be an occurrence of two simultaneous events: (1) reorientation of the molecule; and (2) the presence of a defect site in its vicinity. In the framework of the model, the temperature dependence of the relaxation time can be written in the form:

$$\tau = \tau_0 \exp\left\{\frac{H_a}{kT} + C\exp\left(-\frac{H_d}{kT}\right)\right\} \quad (7)$$

where H_a is the height of the potential barrier of the reorientation of water molecules; H_d is the energy of the defect formation; k is Boltzmann's constant and C is a number inversely proportional to the maximum possible defect concentration, η. The pre-exponential time constant, τ_0, can vary with temperature. The increase in temperature leads, on the one hand, to an increase in the probability of attaining sufficient energy to break the bonds between the reorienting molecule and its neighbors; or, on the other hand, it leads to a decrease in the probability of finding a defect in the vicinity of the moving molecule. The interplay of these two terms yields the appearance of the minimum observed in the temperature dependence of the relaxation time.

The temperature dependences of characteristic times corresponding to the frequency of the maximum of the relaxation loss peak (Figure 11) revealed that saddle-like process II.1 was observed in both kaolinites and montmorillonites (Figure 5), while an additional saddle-like process, II.2, was found only in the Co- and Ni-montmorillonites (Figure 11).

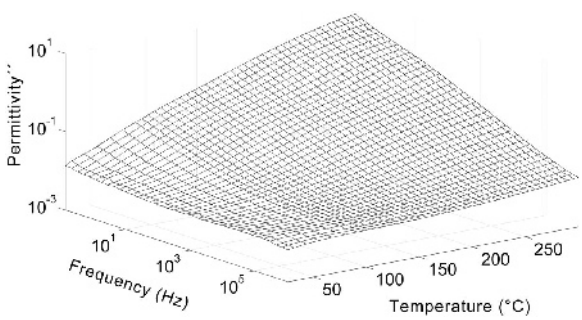

Figure 9. Typical 3D plot of the frequency and temperature dependences of the dielectric losses after annealing the sample for 3 h at 300ºC plotted for Ni-montmorillonite.

As discussed above, two main water-adsorption centers are present in the clay-mineral structure: (1) the basal oxygen atoms and cations trapped in hexagonal holes on the surfaces, and (2) exchangeable interlayer cations. Unlike the low-temperature processes I.1 and I.2 related to the relaxation of ice-like structures, the non-monotonous saddle-like processes, labeled II.1 and II.2 in Figure 5, can be assigned to the relaxation of confined water molecules (Gutina *et al.*, 2003; Feldman *et al.*, 2006). The two types of water structures characterized by different dynamics can coexist and that was recently confirmed by differential scanning calorimetry (DSC) experiments by Kozlowski (2011, 2012). The low-temperature exothermic peaks observed in the DSC measurements show that a significant amount of adsorbed water in clay minerals remains in an unfrozen state when cooling to −70ºC (Kozlowski, 2011, 2012), which confirms and follows the findings of Low *et al.* (1968a,b). The saddle-like relaxation process II.1 is clearly observed for both clay minerals (kaolinites and montmorillonites) and can be assigned to confined water between two interfaces (outer surface of powder granules on one side and air on the other). At the same time, no other saddle-like process II.2 was observed for kaolinites, which means that in the case of montmorillonites an additional source of confinement was present. The interlayer space of montmorillonite structures may have been the source of this extra second confinement. Exchangeable Co^{2+} and Ni^{2+} ions can form ion-water rigid structures in the interlayer gaps while the K^+ ion is known by its strong disordering effect on

Table 4. Calculated activation energies, $E_{I.1}$ and $E_{I.2}$, of the low-temperature relaxation processes (I.1 and I.2) in the montmorillonite samples.

Sample	$E_{I.1}$ (kJ/mol)	$E_{I.2}$ (kJ/mol)
K-montmorillonite	35	31
Co-montmorillonite	49	25
Ni-montmorillonite	55	34

https://doi.org/10.1346/CCMN.2014.0620106 Published online by Cambridge University Press

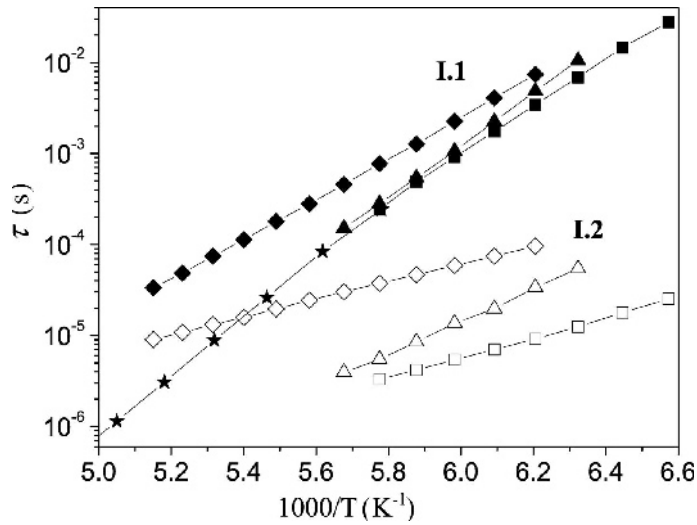

Figure 10. Temperature dependences of the relaxation times of the low-temperature processes for the montmorillonites (◆ K ◇; ■ Co □; ▲ Ni Δ). Filled symbols correspond to the I.1 process, open symbols to the I.2 process. Stars correspond to the temperature dependence of the relaxation time of the low-temperature process in glass (Gutina *et al.*, 2003).

unfrozen interlayer water. Indeed, the K^+ ion is characterized by hydrophobic properties ('negative hydration') at which the lifetime of water molecules to be in the immediate environment of the ion is less than that in the bulk solution (Krestov, 1991; Samoilov, 1957). Hence, the process II.2 is observed only for the Co- and Ni-montmorillonite samples.

The saddle-like process is shown (Figure 11) to depend heavily on the scale at which the relaxation takes place. Characteristic relaxation times for the process II.1 are slower than those for process II.2. The saddle-like behavior was fitted to equation 7 by means of a least-squares fit procedure. The fitting curves show good agreement with the proposed model (Figure 11). The resultant fit parameters are listed in Table 5.

The values of the activation energies H_{a1} and H_{d1} for the process II.1 for all clay minerals under study are in good agreement with the energies of molecular re-orientation and defect formation in confined water (Gutina *et al.*, 2003) but depend on the properties of individual ions. A more detailed investigation is required and may become a subject for further study.

The percolation process

At the mid-temperature range, all of the samples studied demonstrated typical percolation behavior of the

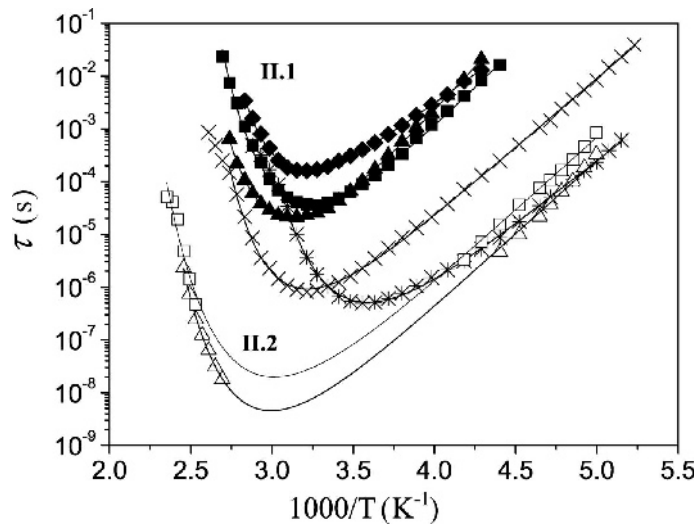

Figure 11. The temperature dependence of the characteristic times of the mid-temperature relaxation processes for montmorillonites (◆ K; □ Co ■; Δ Ni ▲) and kaolinites (* K; × K, Ba). Filled symbols for the montmorillonites correspond to the II.1 mid-temperature process and the open symbols to process II.2. The solid lines are the fitting curves according to equation 7.

https://doi.org/10.1346/CCMN.2014.0620106 Published online by Cambridge University Press

Table 5. Fitting parameters obtained using equation 7.

Sample	Process II.1				Process II.2			
Fit parameter	τ_0 (s)	H_{a1} (kJ/mol)	H_{d1} (kJ/mol)	η	τ_0 (s)	H_{a2} (kJ/mol)	H_{d2} (kJ/mol)	η
K-montmorillonite	2×10^{-12}	43.2	36.0	7×10^{-7}	–	–	–	–
Co-montmorillonite	1×10^{-14}	53.2	41.6	1×10^{-7}	1×10^{-17}	53.0	24.0	7×10^{-5}
Ni-montmorillonite	1×10^{-14}	55.6	42.5	1×10^{-7}	3×10^{-18}	53.2	27.7	2×10^{-5}
K-kaolinite	2×10^{-16}	46.6	26.3	6×10^{-6}	–	–	–	–
K,Ba-kaolinite	6×10^{-16}	50.3	31.6	3×10^{-6}	–	–	–	–

dielectric spectrum as mentioned in the results section above. Such a process was previously associated with the percolation of an apparent dipole moment excitation, within a developed fractal structure of connected pores in a hydrated porous medium (Gutina *et al.*, 2003; Puzenko *et al.*, 1999). Note that the fractal geometry is a mathematical tool for dealing with the complex systems that have no characteristic length scale. Scale-invariant systems are usually characterized by a non-integer (so-called fractal) dimension (Bunde and Havlin, 1995). Similar to porous silica glasses, in the clay minerals the dipole excitation can also be linked to the self-diffusion along random paths of charge carriers within the channels. A transfer of the electric excitation along the developed fractal structure of the connected pores can be described by the normalized dipole correlation function (DCF), $\Psi(t)$. Note that a transfer of the electric excitation through the porous medium can occur even in the case of closed pores which are topologically not connected one to another. However, the distance between the neighboring pores filled with the dielectric or conductive material should be small enough to provide a 'physical' pore coupling *via* the electric interaction. A detailed description of the relaxation mechanism associated with an excitation transfer based on a regular fractal model was introduced by Feldman *et al.* (2006), where it was applied for the cooperative relaxation of ionic micro-emulsions at percolation. Based on percolation theory and the fractal characterization of the clay minerals, the DCF at the percolation threshold was represented by an asymptotic stretched-exponential term (Gutina *et al.*, 2003; Puzenko *et al.*, 1999):

$$\Psi(t) = \exp\left[-\left(\frac{t}{\tau_p}\right)^{D_p/3}\right] \quad (8)$$

where τ_p is an effective relaxation time and D_p is a fractal dimension of the media. In order to determine the value of D_p, the relaxation law (8) can be fitted to the experimental correlation functions. For this purpose the complex dielectric permittivity data were expressed in terms of the dipole correlation function using the Laplace transform.

Dielectric permittivity data were taken at the percolation threshold temperature for all studied samples. The DCF (Figure 12) values were then fitted to equation 8 after applying the Laplace transform. The D_p values obtained are presented in Table 6.

Note that the fractal dimension discussed here is the fractal dimension of the dipole excitation transfer paths connecting the different kinds of hydration centers located on the pore surface. The calculated fractal dimension of the pathways connecting the hydration centers lies between 1 and 2 (Table 6). Due to the relatively small water-content values of all the samples, the water molecules adsorbed by the materials are bound to these centers. The paths of the excitation transfer span the fractal pore surface and 'depict' the backbone of clusters formed by the pores on a scale that is larger than the characteristic distance between the hydration centers. Thus, a fractal dimension of the paths D_p approximates the real surface fractal dimension in the scale interval considered.

The values of the fractal dimension, D_p, of montmorillonites are a little larger than those of kaolinites (Table 6). This fact, as well as the increase in the percolation temperature values (Table 3) for montmorillonites, can be explained by the much more developed surface structure of this type of clay mineral due to the presence of interlayer spaces that are wide compared to kaolinites.

An additional method to quantify the structural information of the clay minerals using a fractal analysis of the SEM images was applied in the present study. Fractal analysis is a powerful approach for quantifying the structure of complex systems which exhibit a measure of self-similarity. Such similarity is usually reflected at different length scales, as discussed in detail

Table 6. Fractal dimensions of the montmorillonite and kaolinite samples.

Sample	D_p	D_f
K-montmorillonite	1.74	1.85
Co-montmorillonite	1.67	1.79
Ni-montmorillonite	1.75	1.80
K-kaolinite	1.48	1.66
K,Ba-kaolinite	1.30	1.81

https://doi.org/10.1346/CCMN.2014.0620106 Published online by Cambridge University Press

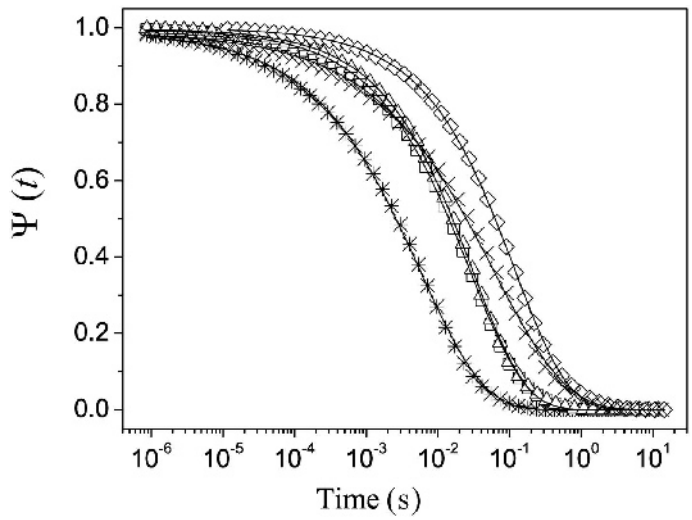

Figure 12. Semi-log plot of the dipole correlation function $\Psi(t)$ for montmorillonites ($\diamond$ K; $\square$ Co; Δ Ni) and kaolinites (* K; $\times$ K, Ba) at the temperatures corresponding to the percolation point. The solid line corresponds to the fit.

by Narine and Marangoni (1999) and by Tang and Marangoni (2006a, 2006b).

In an SEM image the grayscale intensity is proportional to the degree of electron scattering from the sample surface and particularly from areas of differing charge density. Consequently, an analysis of the fractality inherent in the image should reflect the underlying pathways of excitation. The fractality was calculated by counting the number of pixels, $S(N_j)$, in the image with a grayscale from 200 to 255, where the total number of pixels at level j of the recursive coarsening of the image is N_j. For simplicity, N_j was maintained as a power of 2. The detailed description of the calculations can be found in the study by Libster *et al.* (2008). The grayscale is presented below with the cutoff marked (Figure 13).

The image was coarsened by taking the average value of a moving square of four pixels, defining a reduced image. The count was then made again and the process repeated until the image size was too small. Mathematically, this is represented by the expression $N_j = 2^{2(l_{\max}-j)}$, where $l_{\max}$ is the maximum number of recursive stages for the image. A plot was then made in double log scale of the number of counts of white pixels against the image size in pixels.

Power-law behavior was observed and the slopes were calculated from the fitting, according to the relation

$$S(N_j) \propto N_j^D \quad (9)$$

where D is the boundary fractal dimension based on the SEM image depicting the different areas of charge density. This can then be related to the spatial fractal dimension, D_f, by the relationship $D_f = 3 - D$ (Wong and Cao, 1992). The results are summarized in Table 6. The agreement that is evident between these two separate methods of obtaining the spatial fractal dimension points toward the importance of the hydration centers. The D_f values are slightly greater than D_p, as expected, because they describe in more detail the surface structure rather than only the paths connecting the hydration centers.

CONCLUSIONS

Montmorillonites with exchangeable K^+, Co^{2+}, and Ni^{2+} cations and kaolinites with exchangeable K^+ and Ba^{2+} cations were examined by means of Broadband Dielectric Spectroscopy over wide temperature (−121ºC to +300ºC) and frequency (1 Hz−1 MHz) ranges. The rich dielectric spectra can be described in terms of four distributed relaxation processes. Over the low-temperature interval the two Cole-Cole-type dielectric relaxation processes (I.1 and I.2) were observed for montmorillonites only, associated with the interlayer ice-like water molecule relaxations linked to the two types of hydration centers that are located at the hydrophilic centers of interlayer channels (siloxane bonds and trapped cations) and around the interlayer cations.

Figure 13. The gray scale with divisions every eight shades of gray. (The gray scale from white to black, usually varies in 255 shades of gray. For clarity in the figure each division represents the average of eight shades of gray). The cut-off used for the analysis is marked.

https://doi.org/10.1346/CCMN.2014.0620106 Published online by Cambridge University Press

The saddle-like behavior of water adsorbed in the mid-temperature interval has been ascribed to the relaxation of confined water molecules (process II.1). While an additional saddle-like process (II.2) related to the interlayer space confinement was observed for Co- and Ni-montmorillonites only. The absence of the II.2 process for K-montmorillonite is explained by strong disordering effect of the K^+ ion ('negative hydration').

The third relaxation process, occurring in both clay minerals, is associated with percolation of the electric excitation (the self-diffusion of the charge carriers) within the developed fractal structure of connected pores on the outer surface of the granules. The fractal dimensions of the electric excitation paths coming along the pore surface from one hydration center to another are between 1 and 2, consistent with fractal dimension calculated from micrographs for all the samples studied.

ACKNOWLEDGMENTS

The authors thank Prof. I.A. Litvinov and Dr I. Kh. Rizvanov of the A.E. Arbuzov Institute of Organic and Physical Chemistry of the Kazan Scientific Center of Russian Academy of Sciences for their XRF study of aluminosilicates. The authors gratefully acknowledge Dr Yu.N. Osin from the Institute of Geology and Petroleum Technologies of the Kazan Federal University for SEM measurements. The authors also thank Dr V. Uvarov of the H. M. Krueger Center for Nanoscience and Nanotechnology of the Hebrew University of Jerusalem for XRD analyses of the samples. The Israeli authors acknowledge the Israel Science Foundation (ISF), grant number 465/11, for the financial support of the research.

The work was performed in accordance with the Russian Government Program of Competitive Growth of Kazan Federal University.

REFERENCES

Behnsen, J. and Faulkner, D.R. (2011) Water and argon permeability of phyllosilicate powders under medium to high pressure. *Journal of Geophysical Research*, **116**, B12203.

Bunde, A. and Havlin, S. (1995) *Fractals in Science*. Springer-Verlag, Berlin, Heidelberg, New York.

Calvet, R. (1975) Dielectric properties of montmorillonites saturated by bivalent cations. *Clays and Clay Minerals*, **23**, 257–265.

Cole, K.S. and Cole, R.H. (1941) Dispersion and absorption in dielectrics. I. Alternating current characteristics. *Journal of Chemical Physics*, **9**, 341–351.

Feldman, Y., Puzenko, A., and Ryabov, Ya. (2006) Dielectric relaxation phenomena in complex materials. Pp. 1–125 in: *Fractals, Diffusion, and Relaxation in Disordered Complex Systems: a Special Volume of Advances in Chemical Physics* (Y.P. Kalmykov, W.T. Coffey, and S.A. Rice, editors). Volume **133**, part A, Wiley, New York.

Greg, S.J. and Sing, K.S.W. (1967) *Adsorption, Specific Area and Porosity*. Academic Press, London, New York, 303 pp.

Gupta, S.S. and Bhattacharyya, K.G. (2012) Adsorption of heavy metals on kaolinite and montmorillonite: a review. *Physical Chemistry Chemical Physics*, **14**, 6698–6723.

Gutina, A., Antropova, T., Rysiakiewicz-Pasek, E., Virnik, K., and Feldman, Yu. (2003) Dielectric relaxation in porous glasses. *Microporous and Mesoporous Materials*, **58**, 237–254.

Hall, P.G. and Rose, M.A. (1978) Dielectric properties of water adsorbed by kaolinite clays. *Journal of Chemical Society, Faraday Transactions 1*, **74**, 1221–1233.

Hoekstra, P. and Doyle, W.T. (1971) Dielectric relaxation of surface adsorbed water. *Journal of Colloid and Interface Science*, **36**, 513–521.

Ishida, T., Makino, T., and Wang, C. (2000) Dielectric-relaxation spectroscopy of kaolinite, montmorillonite, allophane, and imogolite under moist conditions. *Clays and Clay Minerals*, **48**, 75–84.

Jonscher, A.K. (1996) *Universal Relaxation Law*. Chelsea Dielectrics Press, London, 415 pp.

Kaviratna, P.D., Pinnavaia, T.J., and Schroeder, P.A. (1996) Dielectric properties of smectite clays. *Journal of Physics and Chemistry of Solids*, **57**, 1897–1906.

Kiselev, A.V. (1986) *Intermolecular Interactions in Adsorption and Chromatography*. Vyshzhaya shkola, Moscow (in Russian), 360 pp.

Kozlowski, T. (2011) Low temperature exothermic effects on cooling of homoionic clays. *Cold Regions Science and Technology*, **68**, 139–149.

Kozlowski, T. (2012) Modulated Differential Scanning Calorimetry (MDSC) studies on low-temperature freezing of water adsorbed on clays, apparent specific heat of soil water and specific heat of dry soil. *Cold Regions Science and Technology*, **78**, 89–96.

Kremer, F. and Schoenhals, A. (2002) *Broadband Dielectric Spectroscopy*. Springer-Verlag, Berlin, Heidelberg, New York, 729 pp.

Krestov, G.A. (1991) *Thermodynamics of Solvation: Solution and Dissolution, Ions and Solvents, Structure and Energetics*. Horwood, New York, 570 pp.

Levy, E., Puzenko, A., Kaatze, U., Ben Ishai, P., and Feldman, Yu. (2012) Dielectric spectra broadening as the signature of dipole-matrix interaction. II. Water in ionic solutions. *Journal of Chemical Physics*, **136**, 114503.

Libster, D., Ben Ishai, P., Aserin, A., Shoham, G., and Garti, N. (2008) Microscopic to mesoscopic properties of lyotropic reverse hexagonal liquid crystals. *Langmuir*, **24**, 2118–2127.

Lockhart, N.C. (1980a) Electrical properties and the surface characteristics and structure of clays. I. Swelling clays. *Journal of Colloid and Interface Science*, **74**, 509–519.

Lockhart, N.C. (1980b) Electrical properties and the surface characteristics and structure of clays. II. Kaolinite – a nonswelling clay. *Journal of Colloid and Interface Science*, **74**, 520–529.

Logsdon, S.D. and Laird, D.A. (2002) Dielectric spectra of bound water in hydrated Ca-smectite. *Journal of Non-Crystalline Solids*, **305**, 243–246.

Logsdon, S.D. and Laird, D.A. (2004) Electrical conductivity spectra of smectites as influenced by saturating cation and humidity. *Clays and Clay Minerals*, **52**, 411–420.

Low, P.F., Anderson, D.M., and Hoekstra, P. (1968a) Thermodynamic relationships for soils at or below the freezing point. I. Freezing point depression and heat capacity. *Water Resources Research*, **4**, 379–394.

Low, P.F., Hoekstra, P., and Anderson, D.M. (1968b) Thermodynamic relationships for soils at or below the freezing point. II. Effects of temperature and pressure on unfrozen soil water. *Water Resources Research*, **4**, 541–544

Mamy, J. (1968) Recherches sur l'hydration de la montmorillonite: propriétés diélectriques et structure du film d'eau. *Annales Agronomiques*, **19**, 175–246.

Narine, S.S. and Marangoni, A.G. (1999) Fractal nature of fat crystal networks. *Physical Review E*, **59**, 1908–1920.

Puzenko, A., Kozlovich, N., Gutina, A., and Feldman, Yu.

(1999) Determination of dimensions of pore fractals and porosity of silica glasses from the dielectric dispersion at percolation. *Physical Review B*, **60**, 14348–14359.

Puzenko, A., Ben Ishai, P., and Feldman, Y. (2010) Cole-Cole broadening and strange kinetics. *Physical Review Letters*, **105**, 037601-4.

Puzenko, A., Levy, E., Shendrik, A., Talary, Mark S., Caduff, A., and Feldman Y. (2012) Dielectric spectra broadening as a signature for dipole-matrix interaction. III. Water in adenosine monophosphate/adenosine-5-triphosphate solutions. *Journal of Chemical Physics*, **137**, 194502.

Raythatha, R. and Sen, P.N. (1986) Dielectric properties of clay suspensions in MHz to GHz range. *Journal of Colloid and Interface Science*, **109**, 301–309.

Rotenberg, B., Cadéne, A., Dufrêche, J.-F., Durand-Vidal, S., Badot, J.-C., and Turq, P. (2005) An analytical model for probing ion dynamics in clays with broadband dielectric spectroscopy. *Journal of Physical Chemistry B*, **109**, 15548–15557.

Ryabov, Y., Gutina, A., Arkhipov, V., and Feldman, Yu. (2001) Dielectric relaxation phenomena of water absorbed in porous glasses. *Journal of Physical Chemistry B*, **105**, 1845–1850.

Salles, F., Devautour-Vinot, S., Bildstein, O., Jullien, M., Maurin, G., Giuntini, J.-C., Douillard, J.-M., and Van Damme, H. (2008) Ionic mobility and hydration energies in montmorillonite clay. *Journal of Physical Chemistry C*, **112**, 14001–14009.

Saltas, V., Vallianatos, F., Soupios, P., Makris, J.P., and Triantisc, D. (2007) Dielectric and conductivity measurements as proxy method to monitor contamination in sandstone. *Journal of Hazardous Materials*, **142**, 520–525.

Samoilov, O.Ya. (1957) *The Structure of Aqueous Electrolyte Solutions and the Ion Hydration*. Akademie Nauk SSSR, Moscow (in Russian), 192 pp.

Schaumburg, G. (1994) Overview: Modern measurement techniques in Broadband Dielectric Spectroscopy. *Dielectrics Newsletter*, March issue, 4–7.

Schoonheydt, R. and Johnston, C. (2006) Surface and interface chemistry of clay minerals. Pp. 87–114 in: *Handbook of Clay Science* (F. Bergaya, B. Theng, and G. Lagaly, editors). Volume **1**, Elsevier, New York.

Spanoudaki, A., Albela, B., Bonneviot, L., and Peyrard, M. (2005) The dynamics of water in nanoporous silica studied by dielectric spectroscopy. *The European Physical Journal E: Soft Matter and Biological Physics*, **17**, 21–27.

Sposito, G. and Prost, R. (1982) Structure of water adsorbed on smectites. *Chemical Reviews*, **82**, 553–573.

Tang, D. and Marangoni, A.G. (2006a) 3D fractal dimension of fat crystal networks. *Chemical Physics Letters*, **433**, 248–252.

Tang, D. and Marangoni, A.G. (2006b) Microstructure and fractal analysis of fat crystal networks. *Journal of the American Oil Chemists' Society*, **83**, 377–388.

Tarasevich, Yu.I. (1988) *Structure and Surface Chemistry of Layer Silicates*. Naukova Dumka, Kiev (in Russian), 248 pp.

Tarasevich, Yu.I. and Ovcharenko, F.D. (1975) *Adsorption on Clayey Minerals*. Naukova Dumka, Kiev (in Russian), 351 pp.

Tarasevich, Yu.I. and Ovcharenko, F.D. (1978) A study of the nature of the active centers on the surface of layer silicates. Pp. 138–141 in: *Adsorbents, their Preparation, Properties, and Applications* (in Russian), Nauka, Leningrad.

Tarasevich, Yu.I. and Ovcharenko, F.D. (1980) *Adsorption sur des Minéreaux Argileux*. Institut Français du Pétrole, Rueil Malmaison, Paris, 449 pp.

Vasilyeva, M.A., Gusev, Yu.A., and Shtyrlin, V.G. (2012a) Two types of adsorbed water in natural montmorillonites at low temperatures by dielectric spectroscopy. *Journal of Physics: Conference Series*, **394**, 012027.

Vasilyeva, M.A., Gusev, Yu.A., and Shtyrlin, V.G. (2012b) Differences in behaviour of adsorbed water in kaolinites and montmorillonites in temperature range from −90ºC to +140ºC by dielectric spectroscopy. *Journal of Physics: Conference Series*, **394**, 012028.

Volzone, C., Thompson, J.G., Melnitchenko, A., Ortiga, J., and Palethorpe, S.R. (1999) Selective gas adsorption by amorphous clay-mineral derivatives. *Clays and Clay Minerals*, **47**, 647–657.

Wander, M.C.F. and Clark, A.E. (2008) Structural and dielectric properties of quartz–water interfaces. *Journal of Physical Chemistry C*, **112**, 19986–19994.

Wong, P. and Cao, Q. (1992) Correlation function and structure factor for a mass fractal bounded by a surface fractal. *Physical Review B*, **45**, 7627–7632.

(*Received 28 August 2013; revised 6 February 2014; Ms. 806; AE: M. Plötze*)